

# Rectangular ( $3 \times 2\sqrt{3}$ ) Superlattice of a Dodecanethiol Self-Assembled Monolayer on Au(111) Observed by Ultra-High-Vacuum Scanning Tunneling Microscopy

Lars Müller-Meskamp,<sup>\*,†</sup> Björn Lüssem,<sup>†</sup> Silvia Karthäuser,<sup>†</sup> and Rainer Waser<sup>†,‡</sup>

*Institute of Solid State Research and Center of Nanoelectronic Systems for Information Technology, Research Center Juelich GmbH, 52425 Juelich, Germany, and Institute of Materials in Electrical Engineering and Information Technology 2, RWTH Aachen, Sommerfeldstrasse 24, 52074 Aachen, Germany*

*Received: April 18, 2005; In Final Form: May 12, 2005*

A rectangular ( $3 \times 2\sqrt{3}$ ) surface lattice for long-term-annealed dodecanethiol self-assembled monolayers on Au(111) is observed by ultra-high-vacuum scanning tunneling microscopy. The new lattice has the same density and a unit cell of the same size as the well-known  $c(4 \times 2)$  reconstruction. In contrast, it does not show hexagonal symmetry but rather a sort of thiol pairing, leading to a shift in the binding position of every second molecule. The described structure is believed to be an intermediate phase close to desorption.

Self-assembled monolayers (SAMs) offer an interesting way of creating high-quality organic thin films with tailored electronic and chemical properties. Alkanethiol SAMs on (111)-oriented Au surfaces are probably the best examined SAM system and serve as a model for self-assembly in general. Especially, the molecular structure of the monolayer for different alkane chain lengths has been investigated in great detail.<sup>1,2</sup> During assembly from solution or the gas phase, domains of lying-down surface phases evolve toward a complete saturated monolayer of standing-up molecules. As the molecular lattice of a saturated monolayer, hexagonal packing of the molecules with an additional  $c(4 \times 2)$  symmetry is observed by helium diffraction experiments<sup>3,4</sup> and grazing incidence X-ray diffraction (GIXD).<sup>5</sup> Detailed real-space studies are conducted by scanning tunneling microscopy (STM) and came up with the internal details of the well-known  $c(4 \times 2)$  superlattice,<sup>6</sup> which is formed by alternating heights of the standing-up molecules. Besides this superlattice structure, additional different structures are measured by STM, a  $(6 \times \sqrt{3})$  final phase after long-term storage (6 months),<sup>7</sup> slightly different  $c(4 \times 2)$  phases,<sup>8,9</sup> or a  $(3 \times 4)$  superstructure confirmed by low-energy electron diffraction (LEED) and density functional theory (DFT) calculations<sup>10</sup> as well as different structures from theoretical calculations<sup>11,20</sup> and intermediate standing  $(p \times \sqrt{3})$  phases.<sup>9</sup>

Most experimental studies focus on the assembly process itself and on the structure of a complete monolayer. Long-term evolution or even desorption is studied very little, although the structures emerging in these regimes contribute to the understanding of the SAM system by showing structures and dynamics that are not possible or not visible in a complete monolayer. In this letter, we report about the structure of long-term-annealed SAMs of dodecanethiol on Au(111) examined by ultra-high-vacuum (UHV) STM. In such monolayers with different coexisting phases (Figure 1), a dense, standing-up phase

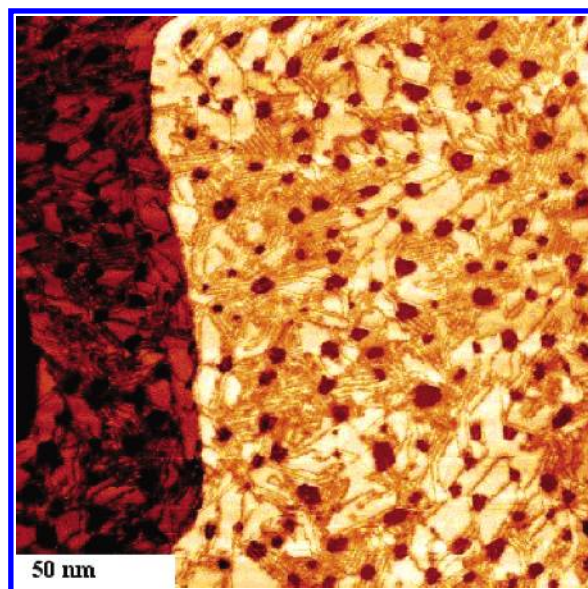


**Figure 1.** STM topography of a dodecanethiol SAM annealed for 6.5 h in solution. The characteristic features of a solution-processed SAM are clearly visible. Besides the substrate step on the left and the small vacancy islands (dark pits), different domains of standing-up (homogeneous areas) and lying-down (striped areas) phases can be distinguished.

with a  $(3 \times 2\sqrt{3})$  superlattice is observed by UHV-STM. For substrates, evaporated (111)-oriented Au thin films on mica with large terraces and very low surface roughness<sup>12</sup> are used. For STM, a JEOL JSPM 4600 UHV-STM with a base pressure of  $3 \times 10^{-10}$  mbar is used with home-made electrochemically etched tungsten tips. (The images obtained were processed by direct current (DC) subtraction followed by line-averaging and contrast adjustments. Figures 1 and 2 are lightly median filtered. No low-pass or fast Fourier transform (FFT) filters were used.) The monolayers are deposited straight from solution, rinsed with ethanol, and directly transferred into the UHV system. A complete, saturated monolayer of dodecanethiols (Aldrich,

\* Author to whom correspondence should be addressed. E-mail: L.Mueller-Meskamp@fz-juelich.de.

<sup>†</sup> Research Center Juelich GmbH.

<sup>‡</sup> RWTH Aachen.

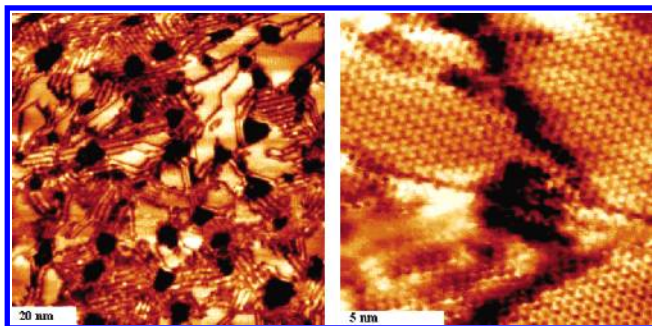


**Figure 2.** STM topography scan of a sample prepared as for Figure 1. On the left, the typical domain structure is visible. When a smaller area in one of the bright, homogeneous domains is scanned, different standing-up phases such as the nonhexagonal ( $3 \times 2\sqrt{3}$ ) phase are clearly visible (right picture).

>97% purity, used as purchased) is formed by exposing the sample surface in 1 mmol/L ethanolic solution for more than 24 h. Afterward, the container with sample and solution is transferred into a hot water bath (77 °C) and annealed for an elongated period. After being annealed, the sample is removed and rinsed with neat ethanol. When the sample is annealed under controlled circumstances with a high concentration of excess thiols available in solution, very large domains of the  $c(4 \times 2)$  phase, limited only by the terrace sizes of the underlying substrate, are formed.<sup>13</sup>

For longer annealing times at elevated temperatures, previously bound thiols are desorbed from the surface due to the shifting balance in the desorption and adsorption process. Thus, surfaces with sub-monolayer coverages of alkanethiols, but with very clean and pronounced molecular structures, are achieved on the sample. In these layers, domains of different densities from lying-down and almost completely desorbed phases up to full-coverage phases with saturated density coexist. In our experiment, the surface coverage of the thiols is reduced over the course of a long annealing process (>6 h) to allow detailed examination of the various resulting phase structures by STM. A topography scan of such layers shows features of the underlying gold substrate as well as features of the SAM itself (Figures 1 and 2). Monoatomic terrace steps are resolved as well as vacancy islands, single-atom-deep depressions in the surface created during the self-assembly process that are visible as dark spots.<sup>6</sup> On the terraces, a mixture of standing-up phases (homogeneous texture) and lying-down phases (striped texture) can be distinguished. The domain boundaries are visible as dark lines.

For full-coverage standing phases, i.e., one molecule per three surface gold atoms or an average area of 0.216 nm<sup>2</sup> per molecule, a new high-density structure with a square superlattice was observed. This structure has the same packing density and even the same unit cell size, as the common  $c(4 \times 2)$  superlattice structure but does not show hexagonal symmetry (Figures 2 and 3). (The  $c(4 \times 2)$  phase can also be expressed as a  $(3 \times 2\sqrt{3})$  phase (Figure 3) but is commonly called  $c(4 \times 2)$  in the literature.<sup>1</sup>) From the Fourier spectrum (Figure 4), the size of the unit cell was measured to be  $8.5 \pm 0.1 \text{ \AA} \times 10 \pm 0.1 \text{ \AA}$  compared to theoretical values of 8.65 and 9.99 Å. This difference is within the accuracy of the STM and partially due to limited software resolution of the FFT spectra. From the surface molecular arrangement, it is generally assumed that all sulfur heads are bound on 3-fold hollow sites forming a commensurate hexagonal lattice.<sup>1,14</sup> For the observed, new structure, this scheme does not fit. Even for the  $c(4 \times 2)$  superlattice, this strict arrangement is questionable. The different

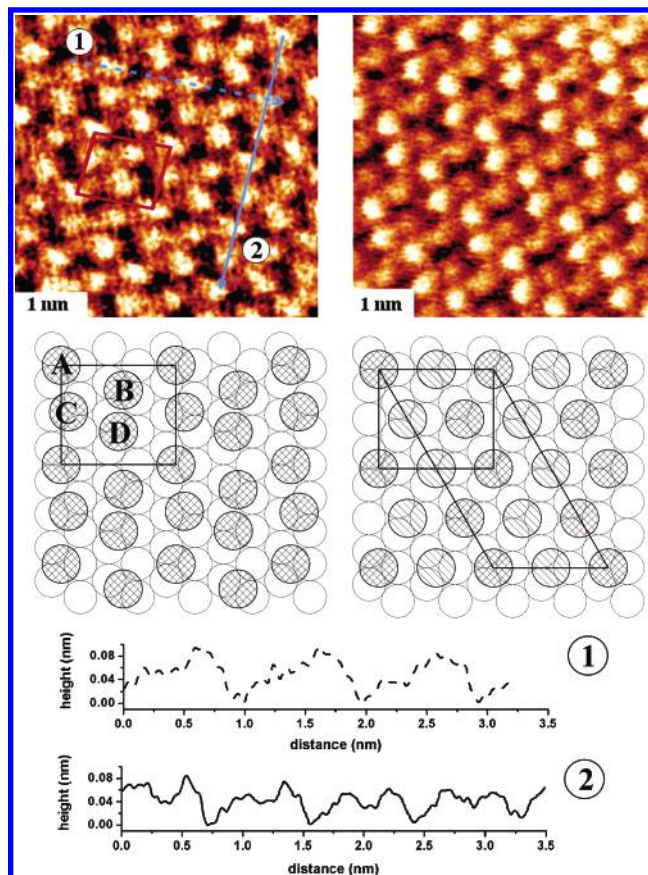


**Figure 3.** On the left side, a STM scan of the nonhexagonal ( $3 \times 2\sqrt{3}$ ) phase and the suggested arrangement of the alkanethiol molecules with respect to the underlying Au(111) lattice. On the right, the well-known  $c(4 \times 2)$  superlattice of alternating heights, which can be named  $(3 \times 2\sqrt{3})$  as well, illustrate the size of the unit cell. The topography profiles A and B taken from the upper-left image show the thiol pairing.

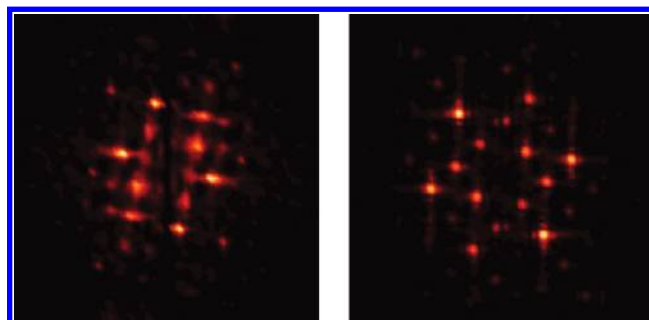


**Figure 4.** Two-dimensional FFT spectra of the  $(3 \times 2\sqrt{3})$  phase (left) and the common  $c(4 \times 2)$  phase (right). Taken from the left spectrum, the base unit cell vector lengths are  $8.5 \pm 0.1 \text{ \AA}$  and  $10 \pm 0.1 \text{ \AA}$  compared to the theoretical values of 8.65 and 9.99 Å of a  $(3 \times 2\sqrt{3})$  unit cell.

apparent heights of the molecules in the  $c(4 \times 2)$  superlattice are claimed to be caused by different twist angles of the molecules and a slight displacement from the hexagonal positions.<sup>1</sup> Another possible explanation is the formation of disulfides on the surface,<sup>15,16</sup> which is contradicted by others.<sup>17</sup> Theoretical calculations of the adsorption energies of alkanethiols on Au(111) are not yet consistent as well. Depending on the exact settings, the energetically most favorable binding site is the hollow,<sup>18,19</sup> the bridge,<sup>20</sup> or the half-bridge site.<sup>21,22</sup>

The positions of the molecules in the observed image cannot be explained by the common 3-fold hollow site placement of the molecules, even if you take skewing and distortion of the images into account. The relative position of the center



molecules in the unit cell does not fit. Thus, we suggest a molecular arrangement as plotted in (Figure 3) for the rectangular ( $3 \times 2\sqrt{3}$ ) structure. The corner molecules (A) are positioned on 3-fold hollow sites at the same positions as in the  $c(4 \times 2)$  structure. To match the observed lattice, two of the center molecules were placed on a bridge (B) and half-bridge (C) position, respectively. Molecule D is on a different 3-fold hollow position. If A is on a hexagonal close-packed site, then D is on a face-centered cubic site and vice versa. This structure evolves during the long thermal annealing process in a thermally changed balance between molecular desorption and adsorption. Upon being cooled, the structure remains in the altered ( $3 \times 2\sqrt{3}$ ) state, which is probably stabilized by the observed molecule pairing, more obvious in the line scans (Figure 3). Thus, we suggest that the described surface phase is an intermediate phase close to desorption. The exact placement, whether molecules B and C (Figure 3) are located on half-bridge or bridge sites is probably beyond the accuracy of the images obtained. But the experimental observation of bridge-site molecules in a densely packed layer offers new insights into the possible configurations of alkanethiol monolayers, showing that the weak energy barriers between the different adsorption sites can be overcome by ordering forces of the alkane chain. Furthermore, the proposed placement reflects a decreased distance between adjacent molecules, like a pairing of two alkanethiols. The observed affinity of the alkanethiols for pairing exists in a  $c(4 \times 2)$  structure as well and may be one of the ordering effects causing the  $c(4 \times 2)$  height modulation.

**Acknowledgment.** We thank K. Szot, S. Kronholz, and H. Haselier for their assistance. Thanks to Nanotec Electronica (<http://www.nanotec.es>) for their WSxM freeware. This work was supported by Deutsche Bundesministerium für Bildung und Forschung under Grant No 13N8361.

## References and Notes

- (1) Schreiber, F. *Prog. Surf. Sci.* **2000**, 98, 151–256.
- (2) Yang, G.; Liu G.-Y. *J. Phys. Chem. B* **2003**, 107, 8746–8759.
- (3) Camillone, N., III; Chidsey, C. E. D.; Liu, G.-Y.; Scoles, G. *J. Chem. Phys.* **1993**, 98, 3503–3511.
- (4) Danisman, M. F.; Casalis, L.; Bracco, G.; Scoles, G. *J. Phys. Chem. B* **2002**, 106, 11771–11777.
- (5) Fenter, P.; Eberhardt, A.; Liang, K. S.; Eisenberger, P. *J. Chem. Phys.* **1997**, 106, 1600–1608.
- (6) Poirier, G. E. *Chem. Rev.* **1997**, 97, 1117–1127.
- (7) Noh, J.; Hara, M. *Langmuir* **2002**, 18, 1954–1956.
- (8) Noh, J.; Hara, M. *RIKEN Rev.* **2001**, 38, 49–51.
- (9) Kobayashi, K.; Yamada, H.; Horiuchi, T.; Matsushige, K. *Jpn. J. Appl. Phys.* **1998**, 37, 6183–6185.
- (10) De Renzi, V.; Di Felice, R.; Marchetto, D.; Biagi, R.; del Pennino, U.; Selloni, A. *J. Phys. Chem. B* **2004**, 108, 16–20.
- (11) Fischer, D.; Curioni, A.; Andreoni, W. *Langmuir* **2003**, 19, 3567–3571.
- (12) Lüssem, B.; Haselier, H.; Karthäuser, S.; Waser, R. *Appl. Surf. Sci.*, in press.
- (13) Bumm, L. A.; Arnold, J. J.; Charles, L. F.; Dunbar, T. D.; Allara, D. L.; Weiss, P. S. *J. Am. Chem. Soc.* **1999**, 121, 8017–8021.
- (14) Ulman, A. *Chem. Rev.* **1996**, 96, 1533–1554.
- (15) Fenter, P.; Eberhardt, A.; Eisenberger, P. *Science* **1994**, 266, 1216–1218.
- (16) Voets, J.; Gerritsen, J. W.; Grimbergen, R. F. P.; van Kempen, H. *Surf. Sci.* **1998**, 399, 316–323.
- (17) Kato, H. S.; Noh, J.; Hara, M.; Kawai, M. *J. Phys. Chem. B* **2002**, 106, 9655–9658.
- (18) Tachibana, M.; Yoshizawa, K.; gawa, A.; Fujimoto, H.; Hoffmann, R. *J. Phys. Chem B* **2002**, 106, 12727–12736.
- (19) Zang, L.; Goddard, W. A., III; Jiang, S. *J. Chem. Phys.* **2002**, 117, 7342–7349.
- (20) Vargas, M. C.; Giannozzi, P.; Selloni, A.; Scoles, G. *J. Phys. Chem. B* **2001**, 105, 9509–9513.
- (21) Cao, Y.; Ge, Q.; Dyer, D. J.; Wang, L. *J. Phys. Chem. B* **2003**, 107, 3803–3807.
- (22) Morikawa, Y.; Liew, C. C.; Nozoye, H. *Surf. Sci.* **2002**, 514, 389–393.